ChemComm

Accepted Manuscript

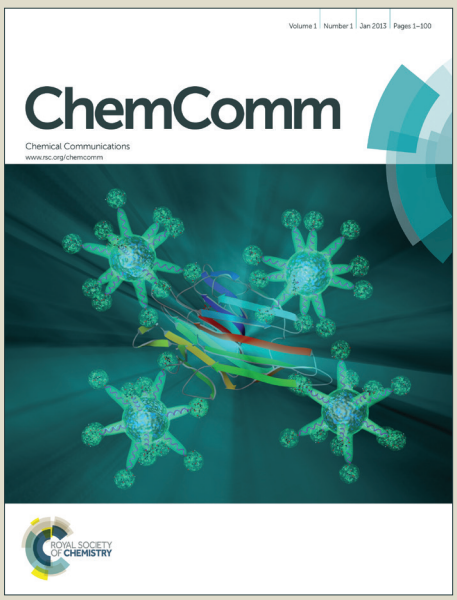

ROYAL SOCIETY OF CHEMISTRY

www.rsc.org/chemcomm

Journal Name

RSCPublishing

COMMUNICATION

Tailor-Made Oxide Architectures Attained by Molecularly Permeable Metal-Oxide Organic Hybrid Thin Films

Cite this: DOI: 10.1039/x0xx00000x

Received 00th January 2012,
Accepted 00th January 2012

DOI: 10.1039/x0xx00000x

www.rsc.org/

Debabrata Sarkar,[a] Dereje Hailu Taffa,[a] Sergey Ishchuk,[a] Ori Hazut,[a] Hagai Cohen,[b] Gil Toker,[a] Micha Asscher,[a] and Roie Yerushalmi*[a]

Tailor-made metal oxide (MO) thin films with controlled compositions, electronic structure, and architectures are obtained *via* molecular layer deposition (MLD) and solution treatment. Step-wise formation of permeable hybrid films by MLD followed by chemical modification in solution benefits from the versatility of gas phase reactivity on surfaces while maintaining flexibility which is more common at the liquid phase.

Metal Oxides (MOs) are the subject of intense research in a number of highly active fields including catalysis, nano-electronics, photonics, optoelectronic devices, sensing, electrochemistry and more.[1,2] MOs are important for such diverse subjects owing to their intrinsic stability, durability, and rich surface reactivity. [3] The stability of MOs which is a useful and attractive characteristic also poses inherent limitations and challenges in achieving fine control of structure and composition in the synthesis of those materials.[4] A versatile approach for tuning oxide composition and properties relies on using molecular precursors as the basic building blocks. Two of the most frequently used methods in this context include sol-gel synthesis[5] and atomic layer deposition (ALD) of oxides,[6] and more recently thermolysis of metal organic frameworks (MOFs).[7] Sol-gel, being a solution based process, provides an elegant synthetic path for entrapment of dopants such as small molecules, inorganic components and metals.[5c] ALD on the other hand is a solvent-free method where the oxide material is constructed in a step-wise manner by vapor phase reactions of small volatile metal precursors reacting with the solid surface, followed by a reaction step with an oxygen source such as water, ozone or other oxidative specie.[6] While Sol-gel presents high flexibility with regard to the oxide composition and entrapped additives, ALD provides control over structural features. Ultimately, it is desirable to introduce a method where both composition and structure of the oxide material can be finely controlled.

Here we present step-wise formation of tailor-made TiO_2 thin films and nanostructures *via* molecular layer deposition (MLD) of organic-inorganic hybrid films followed by liquid phase modification. The hybrid films are easily modified in solution and transformed to the oxide material, yielding programmed doping and architectures. The step-wise formation of the precursor hybrid film by MLD, combined with subsequent chemical modification in solution offers the controllability of surface reactions typical to ALD combined with the flexibility and ability to modify the oxide composition and structure, which is more common at the liquid phase chemistry. As a proof of concept, we demonstrate the tunability of composition, electronic structure, and architecture of TiO_2 structures at the nanometer scale. Key to the tunability of the final metal oxide properties is the hybrid organic-inorganic Ti-EG matrix obtained by MLD of $TiCl_4$ and ethylene glycol (Ti-EG).[8,9] The hybrid film functions as a molecularly permeable, meta-stable layer. The molecular permeability of the Ti-EG films allows permeation of additional components to the entire film volume and thus fine tuning its interactions with the solution phase. We demonstrate tuning of the oxide composition and electronic properties by metal cation adsorption and doping, and selective decoration of core-shell structures (semiconductor core, TiO_2 shell) with noble metal clusters *via* galvanic displacement (GD) and photocatalytic deposition (PD) mechanisms. Recently, we introduced the MLD of Ti-EG films as a route for attaining highly active photocatalytic TiO_2 thin films.[9] The as-deposited Ti-EG MLD layers are amorphous organic-inorganic hybrid films. Upon thermal anneal the organic components decompose and the Ti-O components coalesce and form TiO_2 anatase crystals.[9] Transmission electron microscopy (TEM) showed that films annealed up to 650 ^oC are continuous with coexistence of crystalline TiO_2 (anatase) and an amorphous phase, while films annealed at higher temperatures exhibit crystalline, non-

continuous layers.[9] Here we present a detailed study of the physical properties of Ti-EG films annealed at the intermediate temperature regime using cyclic voltammetry (CV), electrochemical impedance spectroscopy (EIS), temperature-programmed desorption (TPD), UV-VIS spectroscopy, and X-ray photoelectron spectroscopy (XPS).

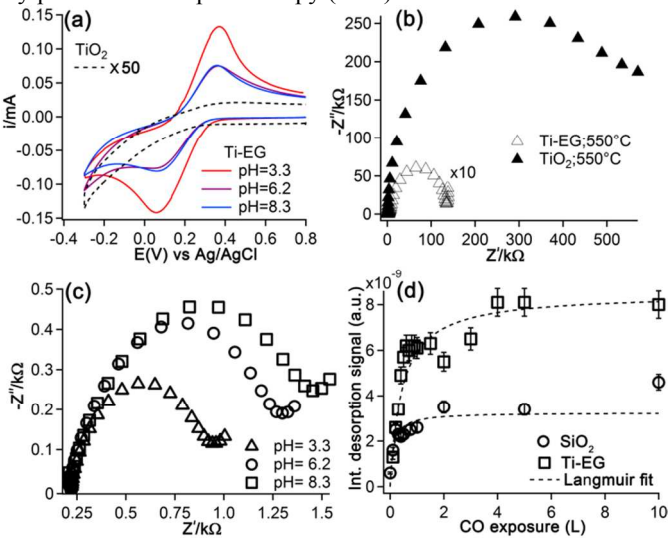

Fig. 1 Comparison of film properties for annealed films prepared by MLD (Ti-EG) and by ALD (TiO_2). (a) CV and (b) EIS plots for ITO electrodes coated with the respective films and annealed at 550 °C. Electrolyte: 2mM $[Fe(CN)_6]^{3-}$ in 0.1 M KCl, (c) EIS plots obtained at indicated pH values for Pt electrodes coated with 40 cycles Ti-EG film and annealed at 650 °C. Electrolyte: 2mM $[Fe(CN)_6]^{3-}$ in 0.1 M KCl. (d) CO uptake measurements vs. exposure isotherms (1 Langmuir (1L)=10^{-6} Torr·sec) (see SI for additional information).

CV measurements of $[Fe(CN)_6]^{3-/4-}$ redox couple obtained for Ti-EG and TiO_2 films prepared by MLD and ALD, respectively, with comparable thicknesses reveal quasi-reversible redox peaks for the former for a range of pH values while no response could be observed for the latter (Fig. 1a). This result suggests that the Ti-EG layers are permeable towards $[Fe(CN)_6]^{3-}$ ions at acidic pH and become less permeable at basic pH. This phenomenon is typical for permeable oxide electrodes and attributed to the local pH of the 'channels' with respect to point of zero charge (pzc) of the oxide.[10] Similarly, EIS measurements and the corresponding Nyquist diagrams demonstrate significant difference in the electronic response of annealed Ti-EG films compared to TiO_2 with charge transfer resistances of ~570 KΩ and ~14 KΩ, for TiO_2 and TiEG films, respectively (Fig. 1b). CV and EIS data for Ti-EG films show an increase in redox current and a decrease in impedance for acidic pH values (Figs. 1a,c). Thus, the electrochemical data demonstrate effective passivation of the electrodes for TiO_2 as expected for ALD, while for Ti-EG the electrodes maintain electronic coupling with the solution. Furthermore, the pH dependent response supports diffusion through 'channels' in contrast to cracks. In addition, TPD was employed for characterizing the surface area of annealed Ti-EG films. TPD allows accurate determination of low surface area thin films and surfaces by measuring the adsorption and desorption kinetics of carbon monoxide (CO) molecules under ultra high vacuum (UHV) conditions. CO-TPD data for Ti-EG film and a SiO_2 reference sample show only a ~3 fold increase in surface area for the Ti-EG films using Langmuir adsorption isotherm model (Fig. 1d). The moderate increase in film surface area further supports our findings that annealed Ti-EG films at the intermediate temperature range are permeable but not porous. Ti-EG films were adsorbed with metal cations from organic and aqueous solutions and characterized by XPS (Figs. 2a,b and SI).

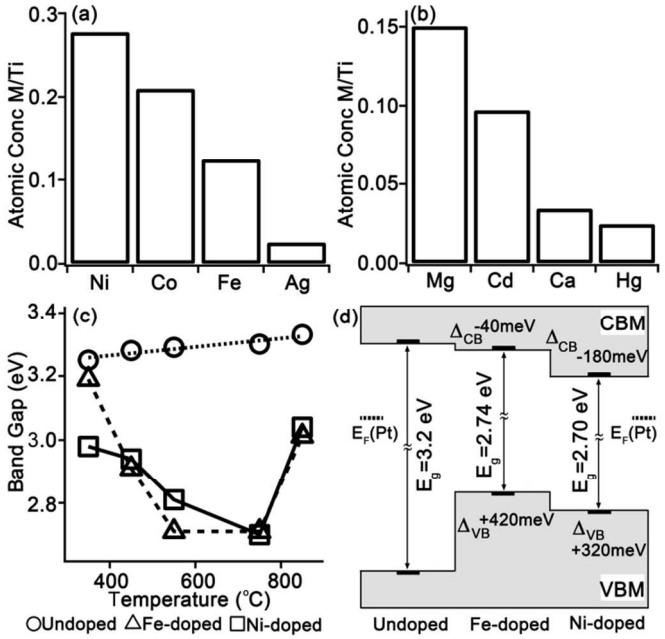

Fig. 2 Doping of Ti-EG films with metal cations. (a) M/Ti atomic ratios for Ni, Co, Fe, Ag, doped Ti-EG adsorbed from organic solutions and annealed at 750 °C. (b) Atomic concentrations for Mg, Cd, Ca, Hg, doped Ti-EG films adsorbed from aqueous solutions and annealed at 750°C. (c) Indirect band gap energies measured for undoped and doped Ti-EG film annealed at different temperatures: Undoped Ti-EG (○); Fe-doped (Δ); Ni-doped (□). (d) VBM and CBM positions of undoped and doped Ti-EG film annealed at 750°C.

Ti-EG films adsorbed with Ni and Fe were annealed at various temperatures and characterized by UV-VIS spectroscopy and XPS. Band gap (BG) values were extracted using Tauc's equation[11] for the undoped, Fe-doped, and Ni-doped films for a range of anneal temperatures (Fig. 2c). A monotonic BG narrowing is obtained for doped films annealed up to 750 °C with lowest BG values obtained for both Fe-, and Ni-doped Ti-EG of 2.74 and 2.70 eV, respectively (see SI section for XRD data and discussion). At higher anneal temperatures BG narrowing is less pronounced, possibly because of segregation of the dopant atoms from the TiO_2 phase at the elevated temperatures. In addition to BG narrowing, valence band maximum (VBM) and conduction band minimum (CBM) positions were determined for doped and undoped samples annealed at 750 °C (Fig. 2d, see Table S1 and SI for additional details). Although Fe-doped and Ni-doped Ti-EG films show similar BG values, the band positions are quite different. For Ni-doped, annealed Ti-EG films, BG narrowing is obtained due to down shift of the CBM (-180 meV) and increase of VBM (+320 meV). In contrast, for Fe-doped, annealed Ti-EG films,

BG narrowing originates mainly from up shift of the VBM (+420 meV) and minor down shift of CBM (-40 meV). The shift in VBM may be attributed to interactions of the O_{2p} state with interstitial metal ions changing the local potential. Furthermore, it is possible for the annealed Ti-EG films that the incorporation of carbon originating from the decomposed ethylene glycol moiety during anneal introduce C_{2p} states, and oxygen vacancies resulting in up-shift of the VBM as well. Thus, the electronic properties of the doped films can be tuned as demonstrated by the BG, CBM, and VBM values.

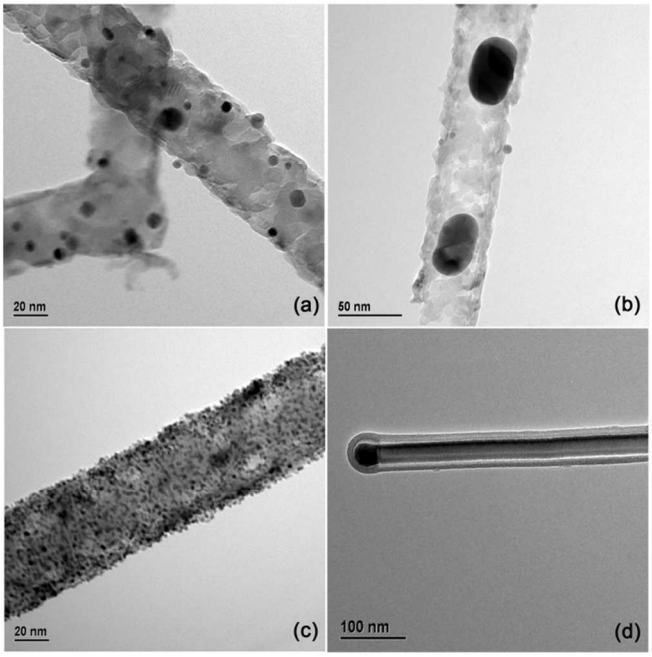

Fig. 3 TEM images of nanostructure architectures obtained by Ti-EG shell formed on NW cores followed by thermal anneal and chemical modification in solution. (a) Gold decoration of the external membrane by photocatalytic deposition obtained under light conditions. (b) Pea pod-like structures obtained by GD reaction with gold carried out in the dark. Synthesis conditions for (a) and (b) were identical except for illumination conditions during gold deposition step (Core: Si NW 30 nm diameter, Shell: Ti-EG 40 cycles, annealed in air, 700 °C, 30 min. Solution modification: $AuCl_3$:HF 1mM:200mM in water for 5 min at the specified illumination condition). (c) Platinum decoration of the external membrane under UV (365nm) illumination (Core: Si NW 30 nm diameter, oxidized in air 700 °C, 30 min, Shell: Ti-EG 40 cycles, annealed in air, 700 °C, 30 min. Solution modification: Etch: HF+H_2O_2 1M solution for 3 min, Metal deposition: H_2PtCl_6 0.5mM + IPA 1% under UV 365nm illumination for 15 min.).
(d) Controlled etching resulting in uniform gap formed between the core and shell owing to the Ti-EG shell permeability (Core: GeO_2 NW 30nm diameter, Shell: Ti-EG 40 cycles, Annealed in air, 350 ^oC 30 min. Solution etch: HF 0.4% + H_2O_2 0.4% in water 1 min.).

Finally, Ti-EG film permeability was used for demonstrating the controlled decoration of core-shell structures with noble metal clusters. Ti-EG films were deposited on NW cores and annealed, followed by immersion in noble metal salt solutions (Figs. 3a-c). Surface decoration with gold clusters is obtained under light while pea-pod like structures are obtained for dark conditions (Figs. 3a,b). The surface decoration is obtained by PD while the pea-pod like structures are obtained under dark conditions as a result of GD reaction between gold cations diffusing through the permeable Ti-EG layer and the NW core and dissolution of the oxidized NW core. PD decoration of Ti-EG tubes is further demonstrated for Pt (Fig. 3c). Facile and uniform etch of GeO_2 coated NWs to form a uniform gap at the Ti-EG shell- NW core interface is another demonstration of utilizing Ti-EG film permeability (Fig. 3d).

Conclusions

MLD is demonstrated as a versatile method for the formation of hybrid nanostructures obtaining controlled electronic structure and rich structural architectures. The deposited Ti-EG hybrid films exhibit molecular permeability properties characterized by electrochemistry in solution and TPD in vacuum. The permeable thin films are further utilized for adsorption of metal cations, doping, and for noble metal decoration of the hybrid structures. Fine control of the annealed oxide electronic structure is demonstrated for band gap as well as band positions. Structural control of hybrid materials is demonstrated by selective decoration by noble metal clusters at the external surfaces by photocatalytic processes and at the internal surfaces by galvanic displacement reaction in the dark.

RY acknowledge financial support from the European Research Council (ERC) under the European Community's Seventh Framework Programme Grant agreement no. 259312, and the Israeli National Nanotechnology Initiative (INNI, FTA project).

Notes and references

[a]Institute of Chemistry and the Center for Nanoscience and Nanotechnology, The Hebrew University of Jerusalem, Jerusalem 91904, Israel. E-mail: roie.yerushalmi@mail.huji.ac.il.

[b]Department of Chemical Research Support, Weizmann Institute of Science, Rehovot 76100, Israel.

†Electronic Supplementary Information (ESI) available: Experimantal details. See DOI: 10.1039/c000000x/

1 F. Caruso, *Adv. Mater.,* 2001, **13**,11.
2 M. G. Kim, M. G. Kanatzidis, A. Facchetti and T. J. Marks, *Nature Materials,* 2011, **10**, 382.
3 A. Agarwala, N. Kaynan, S. Zaidiner and R. Yerushalmi, *Chem. Commun.,* 2014, DOI: 10.1039/C3CC47140C.
4 D. S. Hecht, L. Hu and G. Irvin, *Adv. Mater.,* 2011, **23**,1482.
5 (a) D. Avnir, *Acc. Chem. Res.,* 1995, **28**, 328; (b) J. Livage, M. Henry and C. Sanchez, *Prog. Solid St. Chem.,* 1988, **18**, 259; (c) A. Rutenberg, V. V. Vinogradov and D. Avnir, *Chem. Commun.,* 2013, **49**, 5636.
6 (a) S. M. George, *Chem. Rev.,* 2010**, 110**, 111; (b) M. Leskela and M. Ritala, *Thin Solid Films,* 2002, **409**, 138; (c) M. Knez, K. Nielsch and L. Niinistö, *Adv. Mater.***,** 2007, **19**, 3425.
7. R. Das, P. Pachfule, R. Banerjee, and P. Poddar, *Nanoscale,* 2012, **4**, 591.
8 B. Gong, Q. Peng and G. N. Parsons, *J. Phys. Chem. B,* 2011, **115**, 5930.
9 S. Ishchuk, D. H. Taffa, O. Hazut, N. Kaynan and Roie Yerushalmi, *ACS Nano,* 2012, **6**, 7263.
10 (a) X. Xiang, J. Fielden, W. R. Co´rdoba, Z. Huang, N. Zhang, Z. Luo, D. G. Musaev, T. Lian and C. L. Hill, *J. Phys. Chem. C,* 2013, **117**, 918; (b) A. Calvo, B. Yameen, F. J. Williams, O. Azzaroni and G. J. A. A. Soler-Illia, *Chem. Commun.,* 2009, 2553; (c) H. Taffa, M. Kathiresan, L. Walder, B. Seelandt and M. Wark, *Phys. Chem. Chem. Phys.,* 2010, **12**, 1473.
11 J. Tauc, *Mat. Res. Bull.,*1970, **5**, 721.